

Experimental study of cold plume instability in large Prandtl number Czochralski melt: Parametric dependences and scaling laws



E. Miroschnichenko, E. Kit, A.Yu. Gelfgat*

School of Mechanical Engineering, Faculty of Engineering, Tel-Aviv University, Ramat Aviv, Tel-Aviv 69978, Israel

ARTICLE INFO

Article history:

Received 10 September 2015

Received in revised form

7 November 2015

Accepted 18 December 2015

Communicated by A.G. Ostrogorsky

Available online 2 January 2016

Keywords:

A1. Convection

A1. Fluid flows

A1. Heat transfer

A2. Czochralski method

ABSTRACT

A parametric experimental study of the cold plume instability that appears in the large-Prandtl-number Czochralski melt flows is reported. The critical temperature difference (the critical Grashof number) and the frequency of appearing oscillations were measured for varying Prandtl numbers, aspect ratios of the melt, and crystal/crucible radii ratio. The measurements were carried out by two independent and fully non-intrusive experimental techniques. The results are reported as dimensional and dimensionless parametric dependences, and then are joined into relatively simple empirical relations showing how the critical Grashof number and the frequency of emerging oscillations depend on other parameters.

© 2016 Elsevier B.V. All rights reserved.

1. Introduction

Cold plume instability in the Czochralski model flow was observed first by Munakata and Tanasawa [1], and later by Ozoe et al. [2] in silicone oils with very large Prandtl number, $Pr \geq 1000$. Since liquids with so large Prandtl numbers are not common for crystal growth from melts, these results were not very relevant from a technological point of view. However later, Teitel et al. [3] observed this instability in silicon oils with significantly lower Prandtl numbers, varying from 10 to 100. This range of the Prandtl number is already relevant for growth of different dielectric and optical materials [4], meaning that this type of instability deserves a more detailed experimental and theoretical exploration. The theoretical study of the cold plume instability [9] showed that it can be expected in large-Prandtl number ($Pr > 1$) buoyancy convection flows when convective mixing forms an unstable stratification below a cold upper boundary (the crystal). The instability sets in as oscillations at which the cold liquid first accumulates below the cold crystal and then, when unstable stratification exceeds the critical limit, quickly descends along the symmetry axis. At large supercriticalities this instability results in rather large descending cold liquid volumes called “cold plumes” in [3]. Such instability can appear in melt flow during Czochralski growth of optical and dielectric crystalline materials, whose Prandtl number

varies between 5 and 20 for high melting point oxides [4] and reaches the value of 87 for Bismuth Germanate (BGO) crystals [5].

Our recent experimental and theoretical results on stability of the Czochralski model flow considered all possible instabilities and examined such issues as effect of crystal rotation [6,7], and possibility of non-modal perturbation growth that may lead to an earlier transition from steady to time-dependent flows [8]. In particular, we studied destabilization of the Czochralski model flow by slow crystal rotation, which was explained theoretically in [9]. In most of our previous studies the instability results in cold plumes descending from the crystal surface towards the crucible bottom, but we had no enough experimental data to present a meaningful parametric dependence of critical temperature difference (the Grashof number) on other problem parameters. This issue is addressed in the series of experiments described below.

In the present paper we study how the critical temperature difference of the cold plume instability depends on the Prandtl number, the melt aspect ratio, and the crystal/crucible radii ratio. No rotation effects were included. The experiments are conducted in the facility originally designed by Schwabe [10–12], which was modified by our group to have fully non-intrusive measurements and better control of the system parameters (Fig. 1). Having several tens of measured “critical points”, comprised of the critical temperature difference at which the instability sets in, and oscillation frequency with which the flow starts to oscillate, we follow our recent representation of results as scaling dependences [7]. Namely, we find scaling equations that allow us to combine all the results in two dependences: Grashof number and dimensionless oscillations frequency as functions of the Prandtl number, aspect

* Corresponding author.

E-mail address: gelfgat@tau.ac.il (A.Yu. Gelfgat).

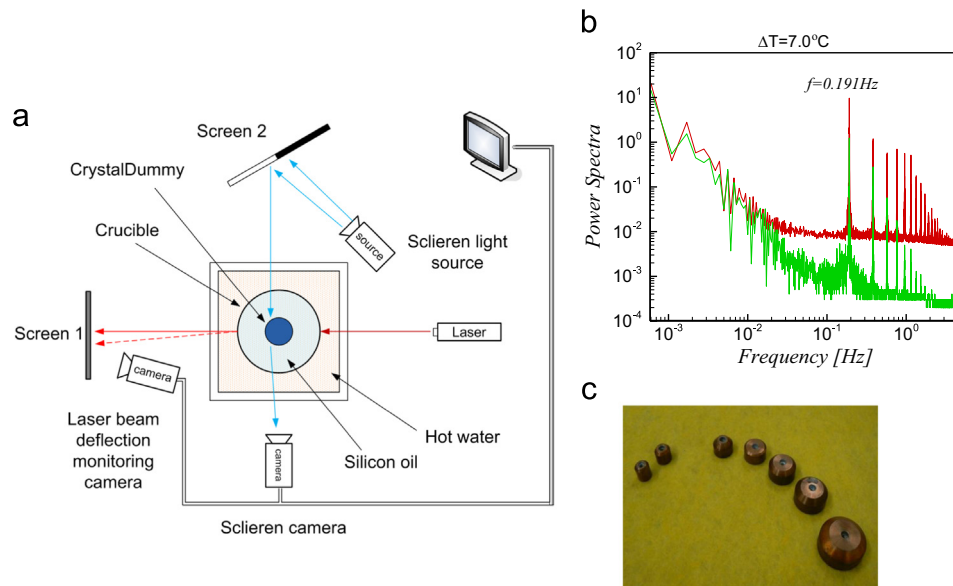


Fig. 1. (a) Sketch of the optical non-intrusive measurements system. (b) Comparison of the frequency power spectra measured by the single laser beam (green) and Schlieren images (red) for the following parameters: $A = 1.5$, $R = 0.7$, $Pr = 57.9$, $\Delta T = 35.4$ °C. (c) Cold crystal dummies of different diameter. (For interpretation of the references to color in this figure legend, the reader is referred to the web version of this article.)

and radii ratios. These dependences can be interpreted as scaling laws, which can be used as “rules of thumb” for estimation of presence or absence of instabilities that can result in appearance of cold plumes in Czochralski growth devices.

2. Experimental setup

The experimental setup is mainly the same as in [3,10–12], to which the reader is referred for more details. The sapphire cylindrical crucible with the radius 20 mm and height 40 mm is placed in the running hot water. The copper crystal dummies (Fig. 1c) of different radii are attached to a copper rod, which is cooled by running cold water. The water temperatures are controlled by the isothermal baths that provide the temperature resolution of 0.1 °C, and additionally by thermocouples placed inside the hot and cold water chambers. In the present experiments the crystal and the crucible do not rotate, so that the flow is governed mainly by buoyancy convection appearing due to the temperature difference between the cold crystal dummy and the hot crucible wall and bottom. The experimental liquids are three silicone oils whose viscosity is 2, 5 and 10 cSt. Their other physical properties are listed in [3].

Compared to the former experimental studies, two main modifications were made. First the special care was taken to measure and control height of the capillary meniscus. For this purpose, we produced a microcontroller-based device with the integrated ADC and digital display. The vertical movement of the axial rod with the attached crystal dummy is monitored by a linear potentiometer whose resistance is converted to millimeters. In all the experiments the meniscus height was kept 1.25 mm, so that the variable meniscus height effect was excluded from the current results. Exploration of this effect requires even more extended set of experimental runs, which we plan to complete in future.

The second modification was completely non-intrusive measurements of the instability onset made by two independent and self-cross-verifying optical techniques. The whole optical system is sketched in Fig. 1. Basing on the comparison between the interferometer and the thermocouple readings reported in [6] and [8], we removed all the thermocouples from the flow under study,

thus eliminating any potential obstacle within the container. Then, taking into account that only frequency of flow oscillations was extracted from the interferometric fringes (see [6,8]), we removed the interferometric setup and replaced it by a single laser beam, deflection of which is monitored as a function of time. The beam passes through the flow and produces a spot on the screen 1. The spot position is stationary when the flow is steady, and oscillates when the flow is time-periodic. Thus, the temperature difference at which the spot starts to oscillate is the critical one. The cylindrical shape of the crucible and the working fluid produce an additional lens effect, increasing additionally the spot deviation in the horizontal direction. The spot position in the horizontal direction is recorded during the whole experiment, so that spectral analysis of its oscillation yields the main frequency and its higher harmonics as is illustrated in Fig. 1b.

For another independent measurement the Schlieren image is created by the light source and black/white screen 2. The varying in time Schlieren images is recorded by the camera and is stored in computer memory with the sampling frequency of 10 fps (frames per second). These images usually are not very informative for the purposes of the flow visualization, however, allow for an independent frequency measurement. Fixing a control window of the size 100×100 pixels, and counting the number of black pixels in it, we obtain an independent, varying in time signal, whose frequency coincides with the frequency of flow oscillations. As is illustrated in Fig. 1b, both measurements yield exactly the same values of the frequency and its higher harmonics.

The measurements were carried out as follows. After a new temperature difference was imposed, we waited 30 min to allow damping of all the transient processes. Then the recording of the beam deflection and Schlieren images started and was done during next 30 min. Data of the last oscillation period was used for calculation of the frequency spectrum. To obtain the critical temperature difference we perform a series of experiments gradually raising the temperature difference by 0.1 °C. The critical temperature difference is obtained after the whole series is post-processed with the obvious accuracy of 0.1 °C. The conclusions below are derived on the basis of approximately 50 measured critical points. On the average, time duration to determine each critical point was 2–3 days.

3. Results

Measured critical temperature differences and critical oscillation frequencies are plotted in Fig. 2 as functions of the crystal dummy radius, for different oils and different oil heights. It is seen that most (but not all) of the dependences are smooth and monotonic, as is illustrated by several dash curves. This allows us to seek for a more general dependence that will join most of the results in a single empirical formula.

Since we are looking for scaling laws connecting the critical temperature difference and critical oscillations frequency with other parameters of the problem, the following analysis is done and the results are reported in the dimensionless form. Since the only characteristic size, which is not varied in the experiments, is crucible radius $R_{crucible}$, it is taken as the characteristic length. The characteristic time, velocity, and pressure are defined as $R_{crucible}^2/\nu$, $\nu/R_{crucible}$, and $\rho\nu^2/R_{crucible}^2$, respectively, where ρ and ν are density and kinematic viscosity of the working liquid. Then the flow is described by the following parameters: the aspect ratio $A = H/R_{crucible}$, the radii ratio $R = R_{crystal}/R_{crucible}$, the Prandtl number $Pr = \nu/\alpha$, the Grashof number $Gr = g\beta\Delta TR_{crucible}^3/\nu^2$, and the Marangoni number $Ma = MnPr$, where $Mn = -\gamma\Delta TR_{crucible}/\rho\nu^2$. Here H is height of the oil in the crucible, $R_{crystal}$ is radius of the crystal dummy, α is the thermal diffusivity, g is the gravity acceleration, β is the thermal expansion coefficient, and $\gamma = d\sigma/dT$ – the parameter describing the dependence of the surface tension coefficient σ on the temperature. The thermophysical parameters of silicone oils, as provided by vendor, can be found in [3].

As it was already discussed in [3] the most problematic is the value of γ . Since the surface tension dependence on the temperature is rather weak, to measure the first significant digit of γ , one needs an accurate measurement of two, and sometimes three, significant digits of the surface tension coefficient σ , which does not seem always affordable. Basing on the data of [3], the ratio Mn/Gr ($= Ma/Ra$, where $Ra = GrPr$ is the Rayleigh number) varies between 0.01 and 0.02. Basing on these data, for the analysis done here we assume that the thermocapillary effect can be neglected. Under this assumption, the Grashof number plays a role of dimensionless temperature difference. For the three oils used in the experiments, the Prandtl and Grashof numbers are $Pr = 23.9$, $Gr = 23540\Delta T$ for 2 cSt oil, $Pr = 57.9$, $Gr = 3450\Delta T$ for 5 cSt oil, and $Pr = 99.2$, $Gr = 785\Delta T$ for 10 cSt oil.

Assuming that the capillary meniscus is attached to the sharp edge of the crystal dummy (as it is observed in the experiments), its shape is defined by three parameters: its height, wetting angle at the crucible wall, and the Bond number $Bo = \rho g R_{crucible}^2/\sigma$. Since the silicone oils density varies between 910 and 950 kg/m³, and surface tension between 19.7 and 19.9 N/m, the Bond number does

not vary noticeably. Thus, keeping height of the meniscus constant, we ensure that the meniscus shape remains almost unchanged in all the experiments. Unfortunately, nothing is known about wetting angle at the three-phase point of a silicone oil, sapphire and air. Our plausible assumption is that this parameter either changes insignificantly for different silicone oils, or does not noticeably affect the instability.

The dimensional experimental data of Fig. 2 is rendered dimensionless and presented in Fig. 3. Placed in the logarithmic scale, most of the dependences tend to be straight lines, as is illustrated in the figure. The dash lines in Fig. 3a and b show power fit of the curves plotted in Fig. 2. Similar exercises with the power fit was made for the dependences of the critical Grashof number and the critical frequency on the other parameters, and most of the results were summarized in the following empirical formula

$$Gr_{cr} \approx (20500Pr^{-1} + 600)R^{0.02Pr-5.8}A^{Pr} \quad (1)$$

$$f_{cr} \approx 0.011Pr^{-0.1}Gr_{cr}^{0.75} \quad (2)$$

Note that in spite of only two governing parameters, the Prandtl number and the critical Grashof number appear in Eq. (2), the critical Grashof number depends on all other parameters via Eq. (1), so that the critical frequency is also a function of all the governing parameters. We observe also that the dependence on the aspect ratio is weaker than on the Prandtl number and the radii ratio. This also can be expected, since cold plume instability arises owing to formation of an unstable thermal stratification below the cold crystal [9], so that the distance from the crystal to the bottom plays a weaker role, at least at the aspect ratios used in the current study.

In Fig. 4 we plot the critical Grashof numbers and critical frequencies divided by the scaling functions (1) and (2) to see how the result deviates from unity. Taking into account experimental uncertainty that always exists, and all the assumptions made, we conclude that above empirical formula yields a good approximation of the results. In particular, we can conclude that the critical oscillations frequency scales as $Pr^{-0.1}Gr_{cr}^{0.75}$. Clearly, some of the points, like the points in the left part of the diagram corresponding to the 10 cSt oil, can deviate from unity simply because they belong to another type of instability, e.g., spoke patterns [13] or oscillating jet [3]. This can be easier checked by computational simulation, rather than experimentally. Results of several previous experimental studies [1,3,6,7] are shown in Fig. 4b by the filled symbols. The critical Grashof numbers obtained in our previous works [3,6,7] fall not very far from Eq. (1) (Fig. 4a). The larger deviation can be due to unknown meniscus height, which was not controlled in those experiments. The critical Grashof number

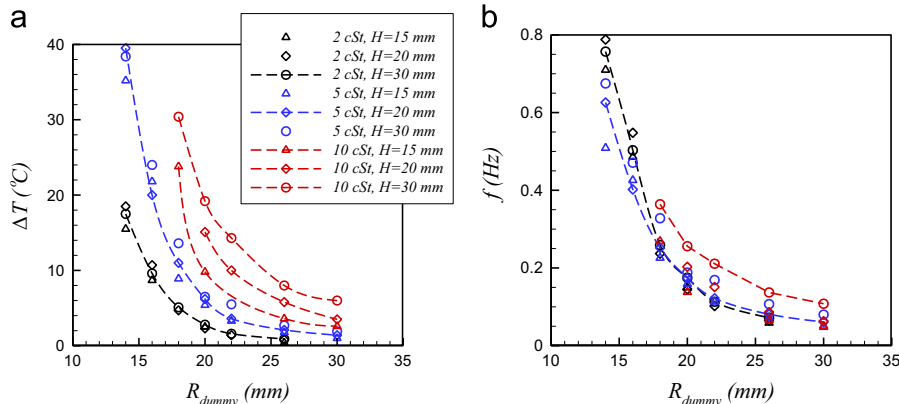


Fig. 2. Measured critical temperature difference (a) and critical frequency (b) versus the crystal dummy radius for different silicone oils and heights above the crucible bottom.

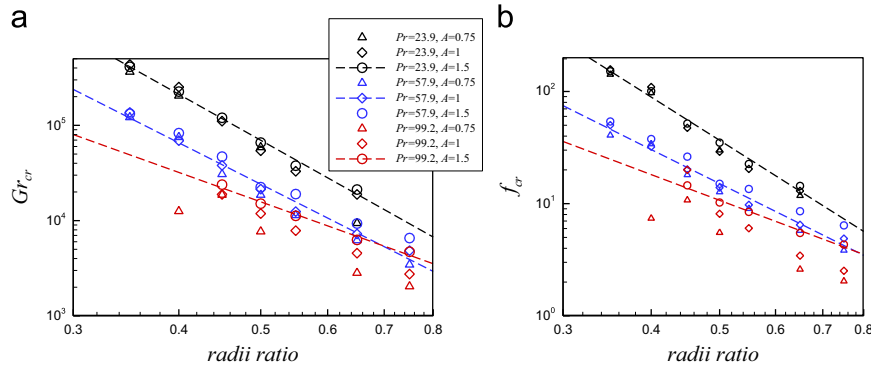


Fig. 3. Measured critical points via dimensionless parameters: the Grashof number (a) and the dimensionless critical frequency (b) versus the radii ratio for different Prandtl numbers and aspect ratios.

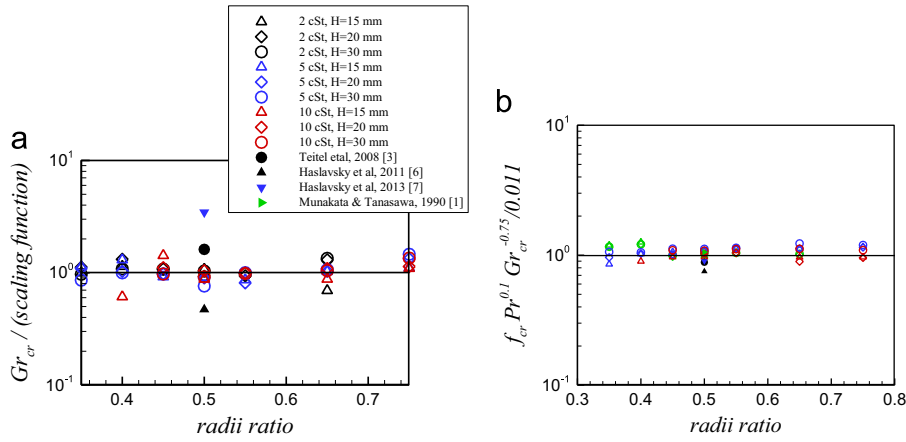


Fig. 4. Scaled critical Grashof number (a) and dimensionless critical frequency (b) versus the radii ratio for different Prandtl numbers and aspect ratios.

measured in [1] is altered by the crystal rotation and necessarily differs from those described by Eq. (1). Surprisingly, the oscillations frequencies reported in all the four papers [1,3,6,7] fit very well to Eq. (2) (Fig. 4b), thus indicating that this relation might be of more general nature. It can be very interesting also to verify the empirical formula by a series of numerical runs, providing that numerically obtained critical values are sufficiently close to the experimental ones.

An empirical equation for the critical Marangoni number can also be derived. To do that we use definition of the Grashof number to extract the parametric dependence of ΔT_{cr} from Eq. (1), and substitute it into definition of the Marangoni number. This results into

$$Mn_{cr} = \frac{Gr_{cr} (-\gamma)}{Bo \beta \sigma}, \quad Ma_{cr} = Mn_{cr} Pr \quad (3)$$

This relation shows that in the case of a weak thermocapillary effect, the critical Marangoni number is the function of the critical Grashof number, the Bond number and the Prandtl numbers, and another dimensionless parameter $\gamma/\beta\sigma$ that depends only on the physical properties of the working liquid. In the case of a strong thermocapillary effect, the empiric relation (1), if exists, should involve also the ratio $Gr/Mn = Ra/Ma$, which, in its turn, is defined by the Bond number and the parameter $\gamma/\beta\sigma$.

4. Conclusions

This experimental study focused on parametric investigation of cold plume instability that appears in the model of large-Prandtl-number Czochralski melt flows. The critical temperature difference (the critical Grashof number) and the frequency of appearing oscillations were measured for the Prandtl numbers varied between 20 and 100, aspect ratios of the melt varied between 0.75 and 1.5, and crystal/crucible radii ratios varied between 0.3 and 0.8. In all the experiments the meniscus height was kept 1.25 mm. The measurements were carried out by two independent and fully non-intrusive experimental techniques.

The results are presented as dependences of either dimensional or dimensionless parameters. It was found that the dimensionless parameter dependences can be approximated by a two relatively simple empirical relations. These relations may serve as a “rules of thumb” for estimation of sub- or supercriticality of flows in Czochralski crystal growth devices.

The results reported can be used also as the experimental benchmark data for computational simulations. The numerical results, in their turn, can validate correctness of the proposed empirical relations and, possibly, improve them.

Apparently, the obtained relations (1) and (2) are applicable only within the considered parameter ranges. They are also incomplete, since they do not account for the dimensionless meniscus height, as well as for possible effects of the Bond number

and the wetting angle at the crucible. It should be stressed that existence of such simple relations is shown for the first time. The extension to other governing parameters and more accurate definition of the applicability ranges can be an objective of future experimental and numerical studies.

Acknowledgments

The authors wish to acknowledge a kind contribution of experimental setup that Professor Dietrich Schwabe donated to our laboratory. This study was supported by the Israel Science Foundation (Grants 426/12 and 408/15) and in part by the Wolfson Family Charitable Trust pr/ylr/18921&18837.

References

- [1] T. Munakata, I. Tanasawa, *J. Cryst. Growth* 106 (1990) 566.
- [2] H. Ozoe, K. Toh, T. Inoue, *J. Cryst. Growth* 110 (1991) 472.
- [3] M. Teitel, D. Schwabe, A. Gelfgat, *J. Cryst. Growth* 310 (2008) 1343.
- [4] D. Klimm, R. Bertram, Z. Galazka, S. Ganschow, D. Schulz, R. Uecker, *Cryst. Res. Technol.* 47 (2012) 247.
- [5] V. Kalaev, Y. Makarov, V. Yuferev, A. Zhmakin, in: H.J. Scheel, P. Capper (Eds.), *Crystal Growth Technology*, Wiley-VCH, Darmstadt, Germany, 2008.
- [6] V. Haslavsky, E. Miroshnichenko, E. Kit, A. Gelfgat, *J. Cryst. Growth* 318 (2011) 156.
- [7] V. Haslavsky, E. Kit, A.Yu. Gelfgat, Experimental modelling of Czochralski melt flow with a slow crystal dummy rotation, *Acta Phys. Pol. Pt. A* 124 (2013) 193.
- [8] V. Haslavsky, E. Kit, E. Miroshnichenko, A.Yu. Gelfgat, *Fluid Dyn. Mater. Process.* 9 (2013) 209.
- [9] A. Gelfgat, *J. Fluid Mech.* 385 (2011) 377.
- [10] P. Hintz, D. Schwabe, *J. Cryst. Growth* 222 (2001) 356.
- [11] P. Hintz, D. Schwabe, H. Wilke, *J. Cryst. Growth* 222 (2001) 343.
- [12] D. Schwabe, *J. Cryst. Growth* 237–239 (2002) 1849.
- [13] A.D.W. Jones, *J. Cryst. Growth* 70–76 (1983) 63.